European Journal of Pharmacology 842 (2019) 306–313

Contents lists available at ScienceDirect

European Journal of Pharmacology

journal homepage: www.elsevier.com/locate/ejphar

Pulmonary, gastrointestinal and urogenital pharmacology

An agonist of a zinc-sensing receptor GPR39 enhances tight junction assembly in intestinal epithelial cells via an AMPK-dependent mechanism

Pawin Pongkorpsakol[a], Chavin Buasakdi[b], Thanyatorn Chantivas[c], Varanuj Chatsudthipong[d], Chatchai Muanprasat[a,d,e,f,*]

[a] Translational Medicine Graduate Program, Faculty of Medicine Ramathibodi Hospital, Mahidol University, Rama VI Road, Rajathevi, Bangkok 10400, Thailand
[b] College of Agricultural and Life Science, University of Wisconsin-Madison, 1450 Linden Dr, Madison, WI 53706, USA
[c] Faculty of Medicine Ramathibodi Hospital, Mahidol University, Rama VI Road, Rajathevi, Bangkok 10400, Thailand
[d] Department of Physiology, Faculty of Science, Mahidol University, Rama VI Road, Rajathevi, Bangkok 10400, Thailand
[e] Excellent Center for Drug Discovery, Faculty of Science, Mahidol University, Rama VI Road, Rajathevi, Bangkok 10400, Thailand
[f] Research Center of Transport Protein for Medical Innovation, Faculty of Science, Mahidol University, Rama VI Road, Rajathevi, Bangkok 10400, Thailand

ARTICLE INFO

Keywords:
Zinc
Intestinal epithelial cells
Tight junctions
AMPK
Barrier function

ABSTRACT

Intestinal barrier function depends on integrity of tight junctions, which serve as barriers to transepithelial influx of noxious substances/microorganisms from gut lumen. The G-protein coupled receptor 39 (GPR39) is a zinc-sensing receptor, which is expressed in several cell types including intestinal epithelial cells (IECs). The main objective of this study was to investigate the effect of GPR39 activation on tight junction assembly in IECs. Treatment with TC-G 1008 (1 μM –10 μM), a GPR39 agonist, and zinc (10 μM –100 μM) increased tight junction assembly in T84 cells. This effect was suppressed by pretreatment with compound C, an inhibitor of AMP-activated protein kinase (AMPK). In addition, western blot analysis revealed that treatment with TC-G 1008 induced AMPK activation in time- and concentration-dependent manners. Interestingly, inhibitors of phospholipase C (PLC) and calcium/calmodulin-dependent protein kinase kinase β (CaMKKβ) abrogated the effect of TC-G 1008 on inducing AMPK activation, tight junction assembly and zonula occludens-1 re-organization. Collectively, this study reveals a novel role of GPR39 in enhancing tight junction assembly in IECs via PLC-CaMKKβ-AMPK pathways. GPR39 agonists may be beneficial in the treatment of diseases associated impaired intestinal barrier function.

1. Introduction

Zinc is a trace element that exerts a variety of physiological effects (Terrin et al., 2015; Tuerk and Fazel, 2009). Interestingly, zinc promotes proliferation and differentiation of intestinal epithelial cells (IECs) (Cohen et al., 2014). Zinc supplement has been shown to improve intestinal barrier function (Y. Shao et al., 2017; Y.X. Shao et al., 2017; Zakrzewski et al., 2017). Moreover, zinc is recommended by the World Health Organization (WHO) to be a crucial part of oral rehydration solution (ORS) (Thiagarajah et al., 2015). Impaired intestinal barrier function contributes to pathogenesis of inflammatory diarrheas and represents a hallmark of inflammatory bowel disease (IBD) (Strober et al., 2007). Importantly, zinc supplement has been demonstrated to attenuate intestinal inflammation in experimental colitis and shorten duration of acute diarrhea (Lamberti et al., 2013; Park et al., 2018). Due to the vital roles of zinc in gut health and diseases, zinc supplement has long been considered as an important micronutrient for alleviating intestinal disorders (Tuerk and Fazel, 2009).

The G-protein coupled receptor 39 (GPR39) has been recognized as a zinc-sensing receptor (Holst et al., 2007). It has been shown to mediate several biological effects of zinc including promoting neuronal functions, enhancing skin wound healing, and improving myogenesis as well as metabolic health (Hershfinkel, 2018). In addition, GPR39 is considered as an anti-depressive drug target (Egerod et al., 2007; Hershfinkel, 2018; Petersen et al., 2011; Peukert et al., 2014; Pongkorpsakol et al., 2017a, 2017b). The GPR39 is primarily coupled with $G_{\alpha q}$ subunit of G protein. Upon being agonized, GPR39 emanates signals mainly via a rise in intracellular calcium concentration ($[Ca^{2+}]_i$) through a $G_{\alpha q}$-phospholipase C (PLC)-inositol triphosphate (IP_3) pathway (Pongkorpsakol et al., 2017a, 2017b). GPR39 is ubiquitously expressed throughout gastrointestinal tract especially on apical membrane of intestinal epithelial cells (Pongkorpsakol et al., 2017a;

* Corresponding author at: Department of Physiology, Faculty of Science, Mahidol University, Rama VI Road, Rajathevi, Bangkok 10400, Thailand.
E-mail address: chatchai.mua@mahidol.ac.th (C. Muanprasat).

https://doi.org/10.1016/j.ejphar.2018.10.038
Received 25 August 2018; Received in revised form 17 October 2018; Accepted 25 October 2018
Available online 26 October 2018

Zakrzewski et al., 2017; Azriel-Tamir et al., 2004; Cohen et al., 2012a, 2012b). GPR39 knockout mice were more susceptible to dextran sodium sulfate (DSS)-induced colitis and had lower expression of tight junction proteins compared with wild-type mice (Sunuwar et al., 2016). Consistently, silencing of GPR39 expression diminished tight junction protein expression in colonocytes (Cohen et al., 2014). However, roles of GPR39 in tight junction assembly and organization are largely unknown. Importantly, TC-G 1008 has recently been identified as a selective agonist of GPR39 (Peukert et al., 2014), which would be useful as a pharmacological tool to elucidate both physiological and pathological roles of GPR39.

AMP-activated protein kinase (AMPK), a heterotrimeric protein complex composed of the catalytic α and regulatory β and γ subunits, acts as an intracellular energy sensor that regulates both cellular and whole-body energy status (Hardie et al., 2016). AMPK is activated by phosphorylation at threonine-172 (Thr-172) of its α subunit by liver kinase B1 (LKB1) or calcium/calmodulin-dependent protein kinase kinase β (CaMKKβ) in response to an increase in AMP/ATP ratio or $[Ca^{2+}]_i$, respectively (Hardie et al., 2016). Apart from its role in controlling energy metabolism, accumulative lines of evidence suggest that AMPK plays an important role in promoting assembly of a tight junction protein ZO-1, a key scaffolding protein required for generating polarity of epithelial cells, in renal epithelial cells (Odenwald et al., 2017; Peng et al., 2009). Nonetheless, the role of AMPK in mediating the effect of GPR39 activation remains unknown. Since $[Ca^{2+}]_i$ is upstream of AMPK, we hypothesized that GPR39 activation may facilitate tight junction assembly in IECs via AMPK activation. Herein, this hypothesis was tested using a selective GPR39 agonist TC-G 1008 and T84 cell monolayers as a model of intestinal epithelia.

2. Materials and methods

2.1. Chemicals

GPR39 agonist, TC-G 1008, was obtained from Tocris Bioscience (Bristol, UK). Inhibitors of AMPK (compound C), CaMKKβ (STO-609), and PLC (U73122) were purchased from Sigma-Aldrich co. (St. Louis, Missouri, USA.). The DMEM F-12 culture medium and fetal bovine serum (FBS) were from Thermo Fisher Scientific Inc. (Waltham, MA, USA). Anti-rabbit antibodies to phospho-AMPK (Thr-172) (p-AMPK), AMPKα, and β-actin were purchased from Cell Signaling Technology (Boston, MA, USA). Anti-mouse antibodies to ZO-1 were obtained from Thermo Fisher Scientific Inc. (Waltham, MA, USA). The horseradish peroxidase- and Alexa Fluor 488-conjugated goat antibodies to rabbit and mouse immunoglobulin G (IgG) were obtained from Abcam (Cambridge, MA, USA.) and Invitrogen (CA, USA), respectively. Other chemicals were obtained from Sigma-Aldrich Co. (Saint Louis, MO, USA) and Calbiochem (San Diego, California, USA). TC-G 1008, compound C, STO-609, and U73122 were dissolved in DMSO. $ZnSO_4$ was dissolved in phosphate-buffered saline (PBS). % DMSO or PBS in cultured medium during treatment was 0.1%.

2.2. Cell culture

T84 cells were obtained from the American Type Culture Collection (Manassas, VA, USA). The cells were cultured in DMEM F-12 medium supplemented with 5% FBS, 100 U/ml penicillin, and 100 μg/ml streptomycin under an atmospheric condition of 95% O_2/5% CO_2 at 37 °C in a humidified incubator.

2.3. Calcium switch assay

The Ca^{2+} switch assay was performed to evaluate tight junction assembly as previously described (Muanprasat et al., 2015; Peng et al., 2009; Pongkorpsakol et al., 2017b). In brief, T84 cells were seeded on a Transwell permeable support (5×10^5 cells/well) (Corning Life Sciences, Tewksbury, MA, USA) and cultured for 7–10 days when TEER was > 1000 Ω cm^2. Disassembly of tight junction was induced by culturing the cells for 16 h in Minimum Essential Medium Eagle Spinner Modification (S-MEM), a Ca^{2+}-free medium. Thereafter, the S-MEM was replaced with a regular medium (DMEM F-12) containing Ca^{2+} (Ca^{2+} switch) in the presence of vehicle or TC-G 1008 (1, 5, 10 μM) with or without signaling inhibitors including compound C (80 μM), STO-609 (5 μM), and U73122 (10 μM). In addition, effect of $ZnSO_4$ (10, 50, 100 μM) on tight junction assembly was investigated. Transepithelial electrical resistance (TEER) was measured before and after (15 min, 30 min, 1 h, 2 h, and 6 h,) a Ca^{2+} switch using the EVOM2 volt-ohm meter (World Precision Instruments, Inc., Sarasota, FL, USA). Percent change of TEER was calculated by comparing TEER measured at each time point to TEER measured before calcium removal.

2.4. Western blot analysis

Protein expression of target signaling was quantitated using western blot method as previously explained (Muanprasat et al., 2015; Pongkorpsakol et al., 2017b). Briefly, T84 cells were seeded on 6-well plates at a density of 1×10^6 cells/well (Corning Life Sciences, Tewksbury, MA, USA) and cultured for 2–3 days before pharmacological treatments. Thereafter, cell lysates were harvested using lysis buffer. Protein concentrations in cell lysates were evaluated using Bradford method (Bradford, 1976). Sixty-microgram protein was loaded and separated using sodium dodecyl sulfate polyacrylamide gel electrophoresis (SDS-PAGE), before being transferred to a nitrocellulose membrane. The membrane-containing protein was blocked for an h with 5% non-fat dried milk (Bio-Rad, Hercules, CA, USA) to prevent non-specific binding of the antibodies and then incubated overnight with rabbit antibodies to phospho-AMPK (Thr-172), AMPKα, or β-actin. The membrane was washed 4 times with Tris-Buffered Saline Tween − 20 (TBST) and incubated for an h at room temperature with horseradish peroxidase-conjugated goat antibodies to rabbit immunoglobulin G (Cell Signaling Technology, Boston, MA, USA). The signals were detected using Luminata™ Forte Western HRP Substrate (Merck Millipore, Billerica, MA, USA). Densitometry analyses were performed using Image J software (version 1.46r, National Institute of Health, Bethesda, MD, USA).

2.5. Immunofluorescence staining

Localization of tight junction protein was investigated using immunofluorescence staining of ZO-1 as previously described (Odenwald et al., 2017; Peng et al., 2009; Yousef et al., 2012). In short, T84 cells were seeded onto the Transwell permeable support (5×10^5 cells/well) and cultured for 10 days before treatment with vehicle, $ZnSO_4$ (100 μM), or TC-G 1008 (10 μM) in the presence or absence of compound C (80 μM) or STO-609 (5 μM). In some experiments, cells were only treated with compound C (80 μM) or STO-609 (5 μM). Two h later, cells were fixed for 10 min with cold methanol (100%) and unspecific binding of antibodies was prevented by incubating for 30 min in a blocking buffer containing 1% BSA, 22.52 mg/ml glycine in PBST (PBS + 0.1% Tween 20). Thereafter, cells were incubated overnight with mouse anti-ZO-1 antibodies at 4 °C. Fixed cells were then washed with PBST and incubated for an h with Alexa Fluor 488-conjugated goat anti-mouse IgG (Invitrogen, CA, USA). The fluorescently labeled ZO-1 was captured by Operetta High-Content Imaging System (Perkin-Elmer, Germany).

2.6. Intracellular Ca^{2+} measurement

Measurement of intracellular calcium or $[Ca^{2+}]_i$ was performed using a Ca^{2+}-sensitive fluorescent indicator indo-1 (Life Technologies, Carlsbad, CA, USA) as previously described (Muanprasat et al., 2015; Sungkaworn et al., 2011). T84 cells were trypsinized and incubated for

an h at 37 °C with 1 mM indo-1. Cells were carefully washed twice with fresh buffers containing 0.441 mM KH_2PO_4, 5.33 mM KCl, 4.17 mM $NaHCO_3$, 5.56 mM D-glucose, 137.93 mM NaCl, 0.338 mM Na_2HPO_4, 1 mM $CaCl_2$ and 1% (w/v) BSA, or the buffer without $CaCl_2$. The mean fluorescent intensity ratios between Ca^{2+}-bound indo-1 (excitation wavelength of 338 nm, emission wavelength of 405 nm) and Ca^{2+}-free indo-1 (excitation wavelength of 338 nm, emission wavelength of 490 nm) were measured by an FP-6200 spectrofluorometer (JASCO, Essex, UK).

2.7. Statistical analysis

The data are presented as means ± S.E.M. Statistical differences between control and treatment groups were analyzed using one-way ANOVA or two-way ANOVA followed by Bonferroni's post hoc test, where appropriate. *n* indicates numbers of repeats. Statistically significant differences are considered when P value was < 0.05. GraphPad Prism software was used for all statistical analyses.

3. Results

3.1. GPR39 agonist and zinc promote tight junction assembly via AMPK

Effects of a GPR39 agonist TC-G 1008 (Peukert et al., 2014) and zinc sulfate ($ZnSO_4$) on tight junction assembly in T84 cells were investigated using a Ca^{2+} switch assay. In this experiment, tight junction re-assembly was induced by re-addition of culture media containing Ca^{2+} (Ca^{2+} switch). Effects of TC-G 1008 and $ZnSO_4$ on tight junction re-assembly were analyzed by a real-time monitoring of TEER after Ca^{2+} switch. We found that TC-G 1008 at 5 μM and 10 μM significantly increased TEER at 30 min to 2 h after treatment in a concentration- and time-dependent manner with a maximal effect being observed at 10 μM (Fig. 1A). $ZnSO_4$ elicited the similar response in a concentration- and time-dependent manner (Fig. 1B). Notably, effects of both stimuli at high concentrations peaked at 2 h after treatment. Consistently, immunofluorescence staining of T84 cells in transmembrane inserts revealed that TC-G 1008 (10 μM) and $ZnSO_4$ (100 μM) accelerated tight junction protein ZO-1 re-distribution to membrane periphery (Fig. 1C).

An involvement of AMPK in mediating the effect of TC-G 1008 and $ZnSO_4$ on tight junction assembly was investigated using compound C, an AMPK inhibitor. Compound C co-treatment significantly abrogated the effect of TC-G 1008 (10 μM) (Fig. 2A) and $ZnSO_4$ (100 μM) (Fig. 2B). As a control, TEER was not affected by the treatment of compound C alone (Fig. 2). Based on the similarities in the kinetic patterns and mechanism of tight junction assembly induced by both endogenous and synthetic agonists of GPR39, it was indirectly implied that beneficial effect of zinc on tight junction assembly might be through GPR39-mediated AMPK activation.

3.2. Effect of GPR39 agonist on AMPK activation

To determine whether GPR39 agonist activated AMPK, time- and concentration-dependent studies of AMPK phosphorylation at Thr-172 within AMPKα subunit, an indicator of AMPK activation, were performed using western blot analysis. We found that TC-G 1008 (10 μM) induced a significant increase in AMPK phosphorylation at 2 h post-

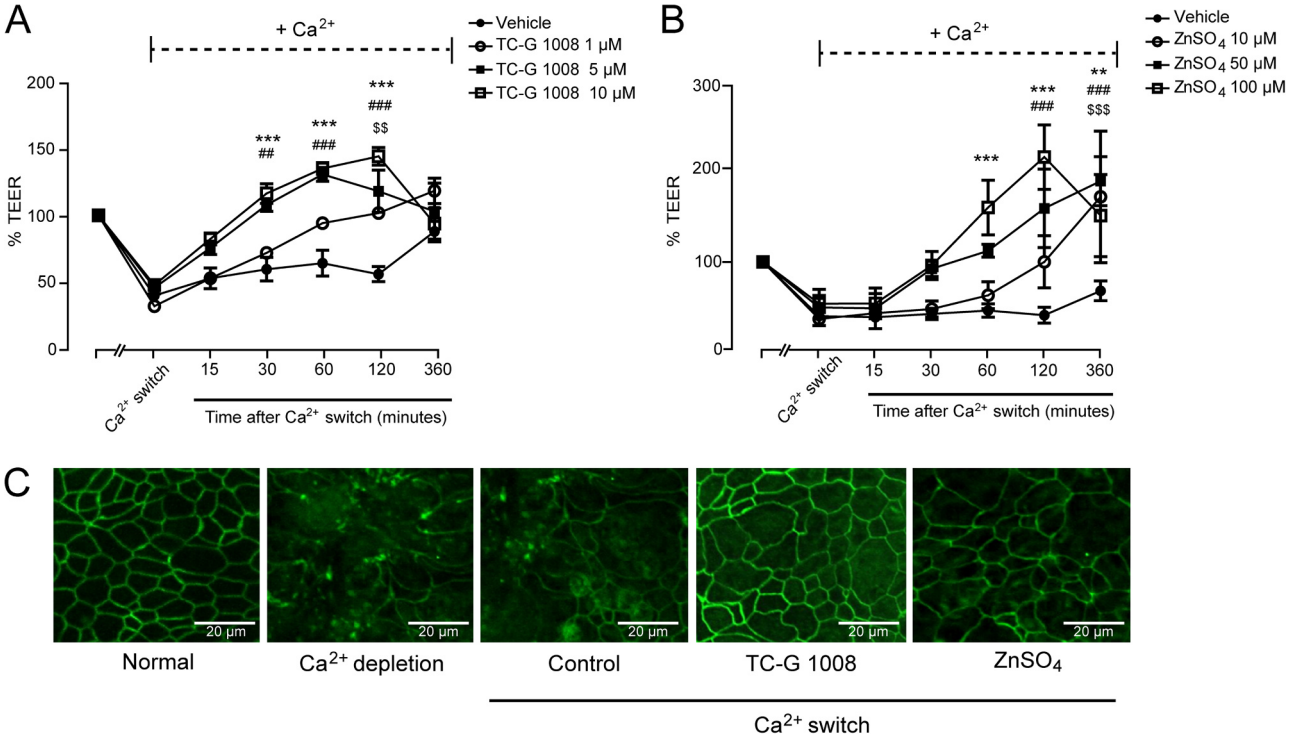

Fig. 1. Effects of GPR39 agonist and $ZnSO_4$ on intestinal barrier function in T84 cells. (A) Effect of GPR39 agonist TC-G 1008 on tight junction assembly analyzed by a Ca^{2+} switch assay. In this experiment, T84 cells were cultured for 16 h in Ca^{2+}-free media. TEER of T84 cell monolayers was measured before and after replacement of Ca^{2+}-free media with media containing Ca^{2+} with or without TC-G 1008. Data are expressed as means of TEER ± S.E.M. (n = 5–7). $^{***}P < 0.001$, TC-G 1008 (10 μM)-treated group compared with vehicle (DMSO) at the same time point. $^{\#\#}P < 0.01$; $^{\#\#\#}P < 0.001$, TC-G 1008 (5 μM)-treated group compared with vehicle at the same time point. $^{\$\$}P < 0.01$, TC-G 1008 (1 μM)-treated group compared with vehicle at the same time point (two-way ANOVA). Pooled values of TEER before Ca^{2+} switch were 2807.66 + 483.53 Ω•cm^2. (B) Effect of $ZnSO_4$ on intestinal barrier function in T84 cells. Data are expressed as means of TEER ± S.E.M. (n = 7). $^{**}p < 0.01$; $^{***}P < 0.001$, $ZnSO_4$ (100 μM)-treated group compared with vehicle (PBS) at the same time point. $^{\#\#\#}P < 0.001$, $ZnSO_4$ (50 μM)-treated group compared with vehicle at the same time point. $^{\$\$\$}P < 0.001$, $ZnSO_4$ (10 μM)-treated group compared with vehicle at the same time point (two-way ANOVA). Pooled values of TEER before Ca^{2+} switch were 2691.4 + 876.47 Ω•cm^2. (C) Immunofluorescence staining of T84 cells in transmembrane inserts showing ZO-1 organization under normal conditions, after Ca^{2+} depletion, and 2 h after Ca^{2+} switch with indicated treatments (vehicle = DMSO).

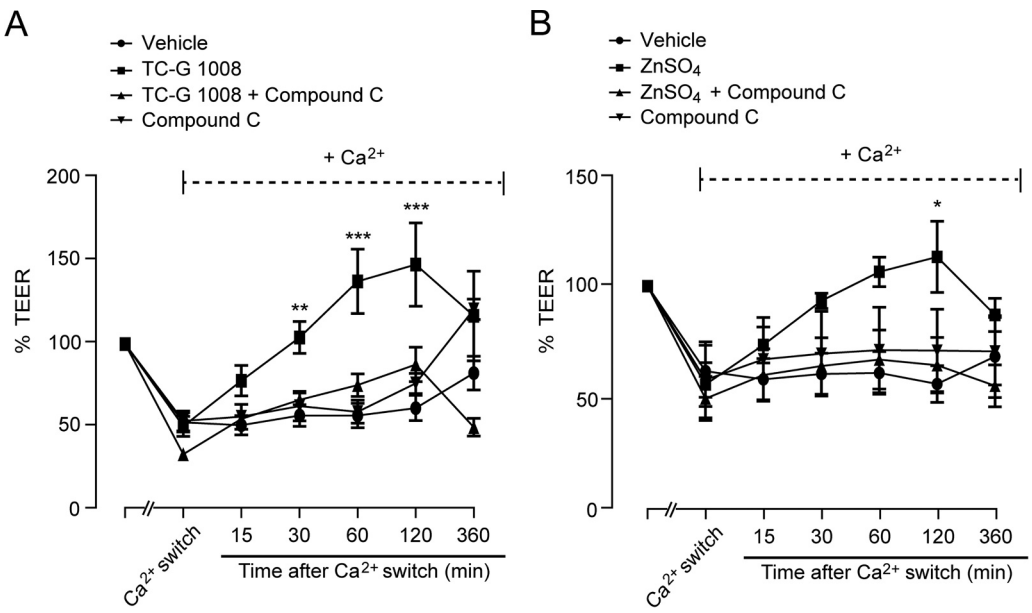

Fig. 2. Involvement of AMPK in the GPR39 agonist- and $ZnSO_4$-induced tight junction assembly. (A) Contribution of AMPK in the GPR39 agonist-mediated tight junction assembly. T84 cells were treated with vehicle, TC-G 1008 (10 μM), TC-G 1008 plus compound C (AMPK inhibitor; 80 μM), or compound C alone. Pooled values of TEER before Ca^{2+} switch were 2749.71 + 697.88 Ω cm^2 (B) Role of AMPK in $ZnSO_4$-induced tight junction assembly. T84 cells were treated with vehicle, $ZnSO_4$ (100 μM), $ZnSO_4$ plus compound C, or compound C alone. Pooled values of TEER before Ca^{2+} switch were 2264.88 + 682.51 Ω cm^2. Data are expressed as means of TEER ± S.E.M. ($n = 9$). $^{*}P < 0.05$; $^{**}P < 0.01$; $^{***}P < 0.001$, TC-G 1008-treated or $ZnSO_4$-treated group compared with vehicle at the same time point (two-way ANOVA).

treatment (Fig. 3A). This time point was further used to investigate the concentration-dependency of TC-G 1008's effect on AMPK phosphorylation. Fig. 3B shows that TC-G 1008 induced AMPK phosphorylation in a concentration-dependent manner with a significant effect being observed at 10 μM. Therefore, this concentration of TC-G 1008 (10 μM) was used in subsequent experiments.

3.3. Effect of GPR39 agonist on intracellular calcium level

GPR39 is a G-protein coupled receptor primarily coupled with $G_{\alpha q}$ and known to transduce signals by eliciting a rise in $[Ca^{2+}]_i$ via a PLC-dependent mechanism (Pongkorpsakol et al., 2017a, 2017b). We next measured $[Ca^{2+}]_i$ using a Ca^{2+}-sensitive fluorescent dye indo-1 to confirm that TC-G 1008 and $ZnSO_4$ stimulate the $G_{\alpha q}$-PLC-Ca^{2+} pathway in T84 cells. As shown in Fig. 4, a fluorescent ratio of Ca^{2+}-bound to Ca^{2+}-free indo-1 (F405/F490) was significantly increased following the treatment with TC-G 1008 (10 μM) and $ZnSO_4$ (100 μM), suggesting that TC-G 1008 and $ZnSO_4$ induced an increase in $[Ca^{2+}]_i$ in T84 cells. Of note, the elevation of $[Ca^{2+}]_i$ induced by TC-G 1008- and $ZnSO_4$ was significantly diminished by pre-treatment with U73122 (10 μM), a PLC inhibitor. These data indicate that TC-G 1008 and $ZnSO_4$ induce an elevation of $[Ca^{2+}]_i$ via $G_{\alpha q}$-PLC pathways.

3.4. Mechanisms of the GPR39 agonist-induced AMPK activation

Since CaMKKβ is downstream to Ca^{2+} signaling, we hypothesized that GPR39 agonist may promote AMPK phosphorylation via Ca^{2+}-CaMKKβ pathway. To prove this hypothesis, western blot analysis of AMPK phosphorylation was performed in T84 cells. As shown in Fig. 5, at 2 h after treatment with TC-G 1008 (10 μM), AMPK phosphorylation was significantly increased compared to control group. Of particular importance, this effect was completely abolished by co-treatment with either a CaMKKβ inhibitor STO-609 or an $[Ca^{2+}]_i$ chelator BAPTA. Neither STO-609 nor BAPTA alone affected AMPK phosphorylation. These results indicate that TC-G 1008 activates AMPK in IECs via Ca^{2+}-CaMKKβ pathway.

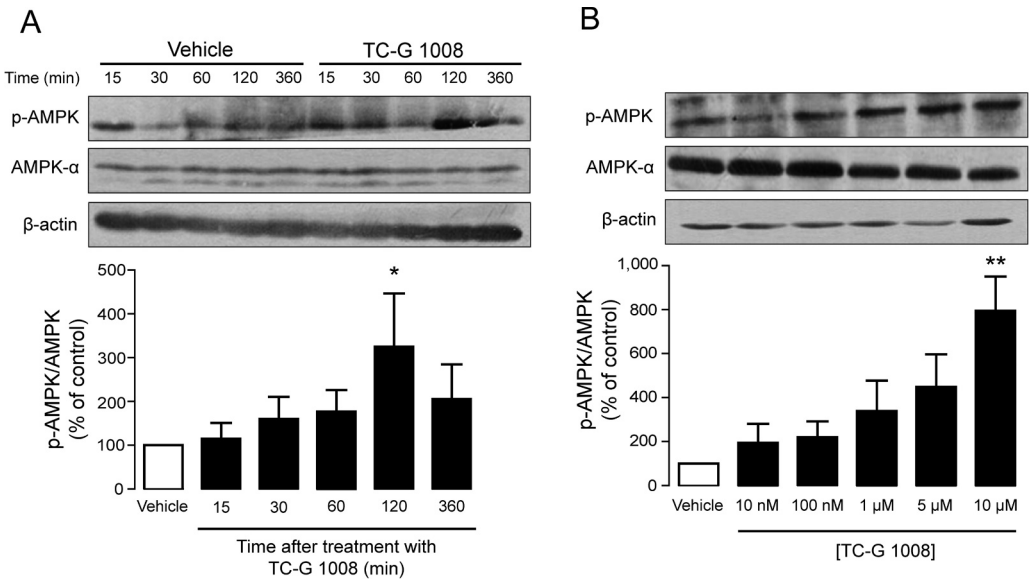

Fig. 3. Effect of GPR39 agonist on AMPK activation in T84 cells. (A) Time course of AMPK activation by TC-G 1008. T84 cells were treated with vehicle or TC-G 1008 (10 μM) for the indicated durations before the sample was harvested for western blot analysis. A representative immunoblot of five independent experiments is shown. (B) Concentration-response of the GPR39 agonist on AMPK activation. T84 cells were incubated with vehicle or TC-G 1008 at the indicated concentrations for 2 h before protein collection for western blot analysis. A representative immunoblot of five independent experiments is shown. Data are analyzed from the ratio of p-AMPK/AMPKα and expressed as % of control (vehicle-treated group), means ± S.E.M. ($n = 5$–7). $^{*}P < 0.05$; $^{**}P < 0.01$, compared with vehicle-treated group (one-way ANOVA).

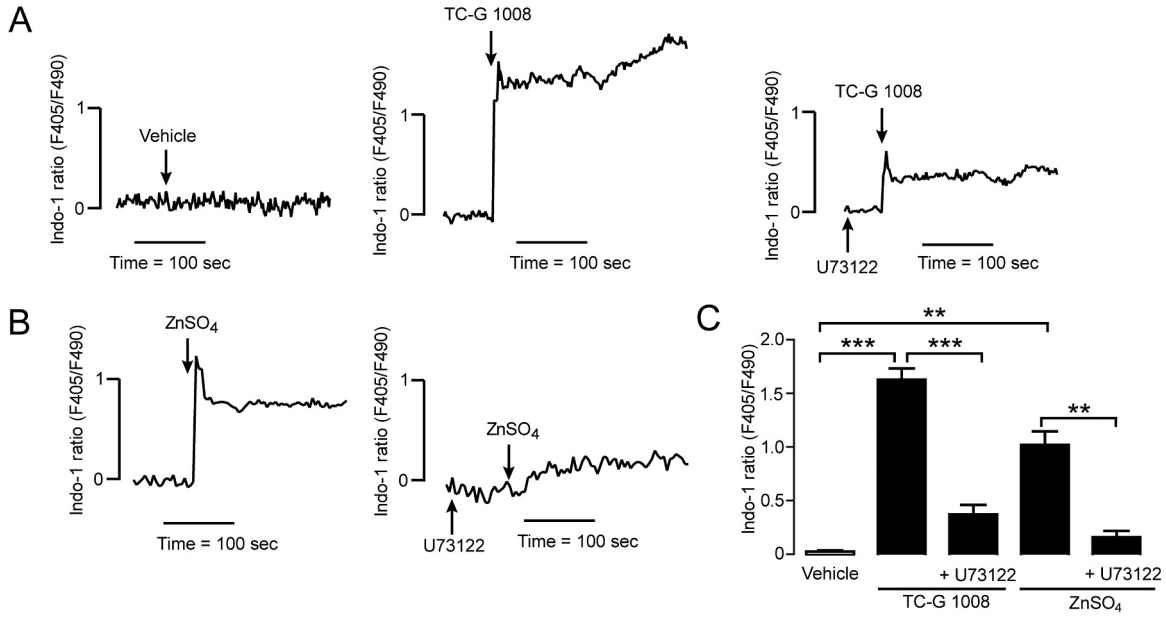

Fig. 4. Effect of GPR39 agonist and $ZnSO_4$ on $[Ca^{2+}]_i$. (A) Representative tracings of indo-1 fluorescence ratio (F405/F490) in response to TC-G 1008 treatment (10 μM) with or without pretreatment with U73122 (PLC inhibitor; 10 μM). (B) Representative tracings of indo-1 fluorescence ratio (F405/F490) following $ZnSO_4$ treatment (100 μM) with or without pretreatment with U73122 (PLC inhibitor; 10 μM). (C) Summary of the data. Data are expressed as means of indo-1 fluorescence ratio (F405/F490) ± S.E.M. ($n = 5$). $^{**}P < 0.01$; $^{***}P < 0.001$ (one-way ANOVA).

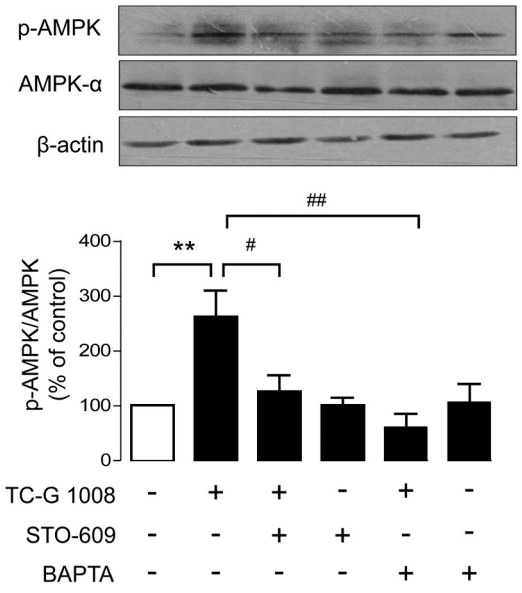

Fig. 5. Involvement of $[Ca^{2+}]_i$ and CaMKKβ in the GPR39 agonist-induced AMPK phosphorylation. T84 cells were pre-incubated for an h with BAPTA (0.2 mM) or STO-609 (5 μM) before exposure to TC-G 1008 (10 μM) for 2 h. Proteins from cell lysates were harvested for western blot analysis. Top, a representative immunoblot from five independent experiments is shown. Bottom, summary of the data. Results are analyzed from the ratio of p-AMPK/AMPKα and expressed as % of control, means ± S.E.M. ($n = 5$). $^{**}P < 0.01$, compared with control group. $^{\#}P < 0.05$; $^{\#\#}P < 0.01$, compared with TC-G 1008-treated group (one-way ANOVA).

3.5. Involvement of PLC and CaMKKβ in the GPR39 agonist-induced tight junction assembly

To confirm that TC-G 1008 induced tight junction assembly via PLC-CaMKKβ pathway, Ca^{2+} switch assays were performed under the conditions of co-treatment with STO-609 (CaMKKβ inhibitor; 5 μM) or U73122 (PLC inhibitor; 10 μM). As depicted in Fig. 6A, STO-609 co-treatment significantly suppressed an increase in TEER induced by TC-G 1008. These results indicate that CaMKKβ is involved in the tight junction assembly induced by GPR39 activation. Likewise, the TC-G 1008-induced TEER increase was significantly suppressed by a PLC inhibitor U73122. These findings suggest that TC-G 1008 induced tight junction assembly in IECs via PLC-CaMKK β pathway.

3.6. GPR39 agonist promotes ZO-1 re-organization

ZO-1 is required for cell polarity and AMPK promotes ZO-1 assembly to the intercellular junctions to establish the epithelial barrier function (Odenwald et al., 2017; Peng et al., 2009). To prove that TC-G 1008 induced ZO-1 assembly, we investigated ZO-1 localization in T84 cells using immunofluorescence staining. Under normal condition of Ca^{2+}-rich media, ZO-1 was located at the cell periphery (Fig. 7A). Depletion of Ca^{2+} in culture media resulted in loss of ZO-1 on cell periphery and ZO-1 translocation to the cytoplasm (Fig. 7A). By 2 h, only partial and sparse re-organization of ZO-1 at the intercellular junctions was established in control group (Fig. 7B). Interestingly, ZO-1 re-localization to the intercellular junctions was more prominent with TC-G 1008 treatment (10 μM) (Fig. 7B). The effect of TC-G 1008-induced ZO-1 re-assembly was disturbed with either compound C or STO-609 co-treatment (Fig. 7C). It was also found that compound C or STO-609 alone did not affect ZO-1 localization (Fig. 7D). These results suggest that TC-G 1008 improves barrier function in IECs, at least in part, by accelerating assembly of ZO-1 to the intercellular junction via CaMKKβ-AMPK-dependent pathways.

4. Discussion

In the present study, we delineated the role of a zinc-sensing receptor GPR39 in the regulation of barrier function in IECs (T84 cells). Functional analyses using TEER measurement revealed that activation of GPR39 improved intestinal barrier function via an AMPK-dependent mechanism. Activation of AMPK by the GPR39 agonist was prevented by the co-treatment with CaMKKβ inhibitor and Ca^{2+} chelator, suggesting the contribution of Ca^{2+}-CaMKKβ signaling in the GPR39-mediated AMPK activation. Furthermore, inhibitors of AMPK, CaMKKβ, and PLC suppressed the effect of GPR39 agonist-induced tight junction

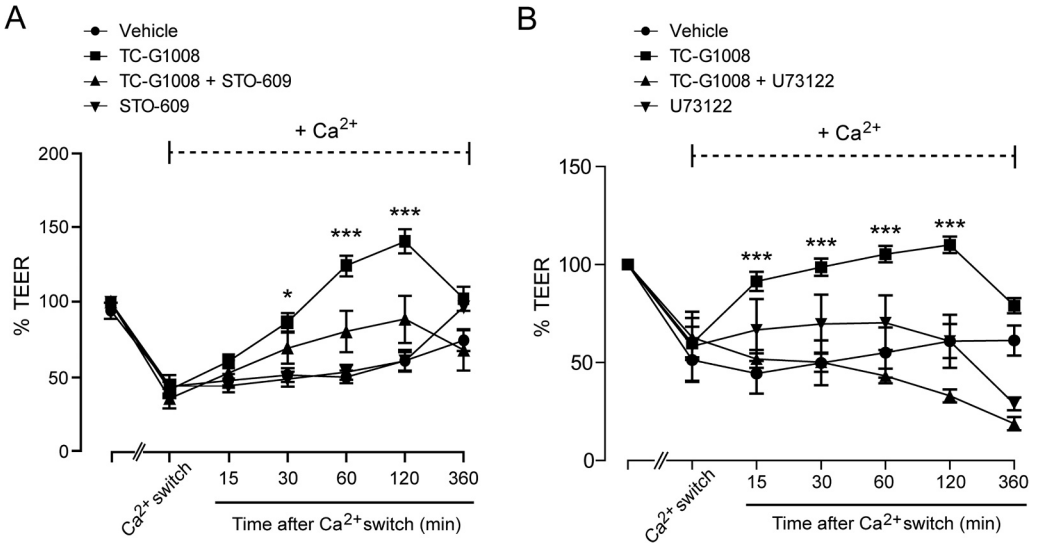

Fig. 6. Involvement of CaMKKβ and PLC in the GPR39 agonist-induced tight junction assembly. (A) Role of CaMKKβ in the GPR39 agonist-induced tight junction assembly. T84 cells were treated with vehicle, TC-G 1008 (10 μM), TC-G 1008 plus STO-609 (CaMKKβ inhibitor; 5 μM), or STO-609 alone. Pooled values of TEER before Ca^{2+} switch of the experiments were 3299 + 410.86 Ω•cm^2. (B) Role of PLC in the GPR39 agonist-induced tight junction assembly. T84 cells were treated with vehicle, TC-G 1008 (10 μM), TC-G 1008 plus U73122 (PLC inhibitor; 10 μM), or U73122 alone. Pooled values of TEER before Ca^{2+} switch of the experiments were 3182.5 + 387.21 Ω cm^2. Data are expressed as means of TEER ± S.E.M. ($n = 5$). $^{*}P < 0.05$; $^{***}P < 0.001$, TC-G 1008-treated group compared with vehicle at the same time point (two-way ANOVA).

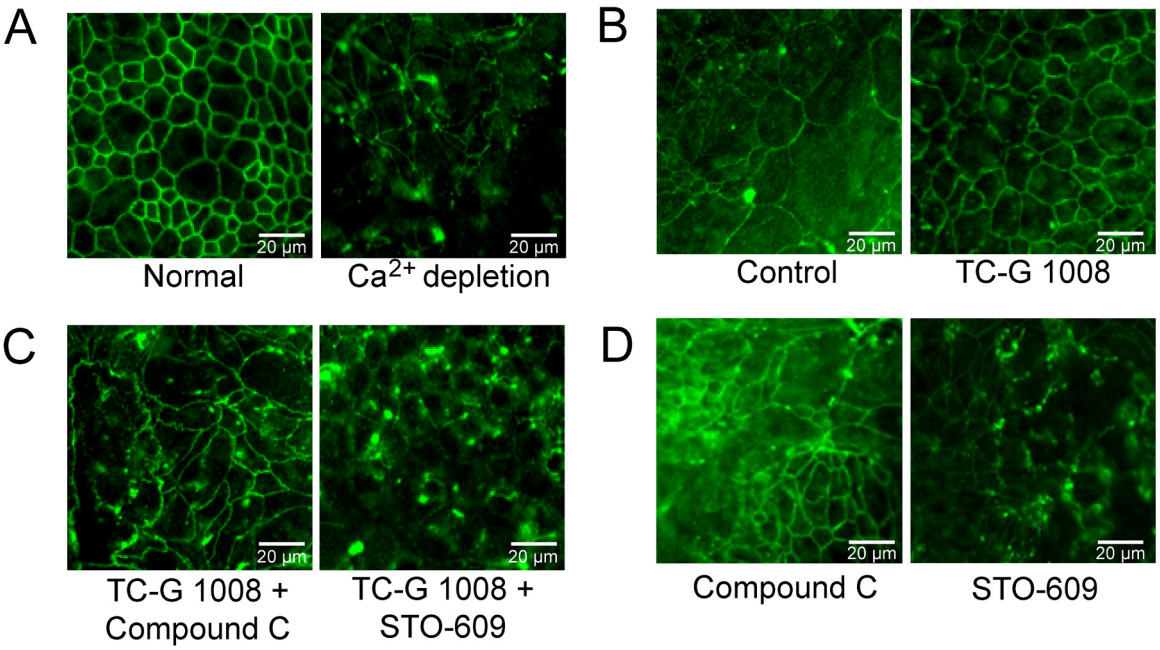

Fig. 7. Effect of GPR39 agonist on ZO-1 re-organization in T84 cells. ZO-1 was stained after calcium switch assays under indicated conditions. (A) ZO-1 distribution under normal condition and Ca^{2+} depletion. (B) ZO-1 distribution after 2 h of Ca^{2+} switch with or without TC-G 1008 treatment (10 μM). (C) Effect of AMPK inhibitor (compound C; 80 μM) and CaMKKβ inhibitor (STO-609; 5 μM) on the TC-G 1008-induced ZO-1 re-distribution after 2 h of Ca^{2+} switch in T84 cells. (D). Effect of compound C and STO-609 on ZO-1 organization after 2 h of Ca^{2+} switch. At least 20 fields of each experiment were captured. Representative images are shown ($n = 3 - 5$).

assembly. Lastly, activation of GPR39 promoted re-assembly of ZO-1 to the intercellular junction in CaMKKβ and AMPK-dependent manners.

Impaired intestinal barrier function is associated with several intestinal diseases including IBD and diarrhea (Hering et al., 2012; Satitsri et al., 2016; Strober et al., 2007). Zinc supplement has been known to exhibit anti-inflammatory and anti-diarrheal effects (de Queiroz et al., 2014; Lamberti et al., 2013; Park et al., 2018). Interestingly, zinc deficiency has been demonstrated to be associated with increased susceptibility to infectious diarrhea and increased degree of severity (Agarwal et al., 2018; Bolick et al., 2014; Lindenmayer et al., 2014). The mechanisms underlying these observations have been debated (Bolick et al., 2018; Patel et al., 2011; Thiagarajah et al., 2015). We found that activation of GPR39 by $ZnSO_4$ or a synthetic agonist TC-G 1008 improved intestinal barrier function in a similar time course. In addition, both $ZnSO_4$ and TC-G 1008 increased TEER in a time-dependent manner with the maximal effect being obtained at 2 h after treatment. These findings suggest that GPR39 mediates the effect of zinc on improving intestinal barrier function. Indeed, western blot analysis revealed that the GPR39 agonist induced AMPK activation within 30 min of exposure. This result is consistent with the previous reports showing the AMPK activation via G protein coupled receptor-mediated $[Ca^{2+}]_i$ elevation (Kim et al., 2015; Muanprasat et al., 2015). Of particular interest, increased TEER and AMPK phosphorylation induced by the GPR39 agonist TC-G 1008 was dramatically declined at 6 h. This might be due to the Rho kinase-dependent receptor internalization, which is a unique characteristic of GPR39 desensitization

upon its activation (Shimizu et al., 2017). In addition, the GPR39 agonist concentration-dependently enhanced TEER and AMPK activation. Of note, $ZnSO_4$ and TC-G 1008 at all concentrations used in this study have been reported to be non-toxic and specific for GPR39 stimulation (Cohen et al., 2014; Holst et al., 2007; Lodemann et al., 2013; Moran et al., 2016; Ni Shuilleabhain et al., 2004; Pavlica et al., 2009; Peukert et al., 2014; Yasuda et al., 2007). In agreement with results from previous studies, potency of TC-G 1008 in improving TEER was approximately 10-fold higher than that of $ZnSO_4$ (Peukert et al., 2014; Y. Shao et al., 2017; Y.X. Shao et al., 2017). These findings indicate that GPR39 mediates the effect of zinc in improving intestinal barrier function and GPR39 stimulation leads to AMPK activation.

AMPK is involved in the GPR39 agonist-induced enhancement of tight junction reassembly. Both zinc supplementation and GPR39 agonists have been reported to be involved in the secretion of glucagon-like peptide 1 and metabolic regulation. Furthermore, GPR39 is preferentially coupled with $G_{\alpha q}$, which is known to activate metabotropic signals including AMPK (Cote et al., 2015; Duca et al., 2015; Muanprasat et al., 2015; Petersen et al., 2011; Peukert et al., 2014; Pongkorpsakol et al., 2017a, 2017b). AMPK is recognized as a key regulator of tight junction assembly in both intestinal and renal epithelial cells (Muanprasat et al., 2015; Peng et al., 2009; Pongkorpsakol et al., 2017b; Zhang et al., 2006; Zheng and Cantley, 2007). Using molecular and pharmacological approaches, we found that GPR39 stimulation induces AMPK activation via a $G_{\alpha q}$-PLC-Ca^{2+}-CaMKKβ-dependent pathway. Likewise, our results suggest that this pathway contributes to ZO-1 re-organization to the intercellular junction following GPR39 activation. Indeed, previous studies demonstrated that AMPK induced ZO-1 re-assembly and improved intestinal barrier function via mechanisms involving myosin light chain kinase (MLCK) inhibition and PKCβ2 activation (Miao et al., 2016; Peng et al., 2009). In addition, AMPK has been shown to activate the newly identified effector G-alpha interacting vesicle associated protein (Girdin) and orchestrate microtubules to tight junction by phosphorylating cingulin, both of which promote and stabilize tight junction integrity (Aznar et al., 2016; Yano et al., 2013).

Since GPR39 is mainly expressed in the tissues where zinc turnover takes place including intestine and defect in GPR39 signaling or zinc homeostasis causes pathological events, it has been postulated that GPR39 activation might have therapeutic benefit. This study not only identified the novel role of GPR39 on tight junction assembly, but also shed some light on its mechanistic insight. We provided evidence that AMPK, which is an intracellular energy sensor, plays a role in mediating the effect of GPR39 activation on enhancing intestinal barrier function. In fact, AMPK has previously been reported to suppress NF-κB-mediated inflammation via PGC-1α, SIRT1, Forkhead box O, and p53 pathways (Chi et al., 2011; Pongkorpsakol et al., 2017b; Salminen et al., 2011). Nevertheless, the effects of GPR39 agonists on NF-κB signaling and intestinal inflammation has never been explored. Since impaired intestinal barrier is known to be an initial pathogenic event of intestinal inflammation-associated diseases, effect of GPR39 agonists on intestinal barrier under inflammatory conditions such as those found in inflammatory diarrheas and IBD should be further investigated.

5. Conclusion

Engagement of zinc-sensing receptor GPR39 exerts the regulatory role on tight junction assembly in IECs via an AMPK-dependent mechanism. Moreover, AMPK activation by GPR39 stimulation is via $G_{\alpha q}$-PLC-Ca^{2+}-CaMKKβ pathway. Therefore, GPR39 represents an important regulator of intestinal barrier function. GPR39 agonists may be of therapeutic utility in the treatment of diseases associated with intestinal barrier disruption.

Acknowledgements

This work is supported by a grant from the Thailand Research Fund (TRF) and Mahidol University (grant BRG5980008). Financial support from the NSTDA Chair Professor grant (the Fourth Grant) of the Crown Property Bureau Foundation and the National Science and Technology Development Agency and the Faculty of Science Mahidol University are also gratefully acknowledged.

CRediT author statement

Pawin Pongkorpsakol: Methodology, Investigation, Formal Analysis, Data Curation, Writing – Original Draft, Visualization. **Chavin Buasakdi:** Investigation. **Thanyatorn Chantivas:** Investigation. **Varanuj Chatsudthipong:** Formal Analysis. **Chatchai Muanprasat:** Conceptualization, Validation, Resources, Writing – Review & Editing, Visualization, Supervision, Project Administration, Funding Acquisition

References

Agarwal, A., Gupta, N.K., Upadhyay, A., Soni, R.K., Shah, D., Jaiswal, V., 2018. Serum zinc levels as a predictor of severity of acute diarrhea. Indian J. Pediatr. 85 (3), 179–183. https://doi.org/10.1007/s12098-017-2493-z.

Aznar, N., Patel, A., Rohena, C.C., Dunkel, Y., Joosen, L.P., Taupin, V., Ghosh, P., 2016. AMP-activated protein kinase fortifies epithelial tight junctions during energetic stress via its effector GIV/Girdin. Elife 5. https://doi.org/10.7554/eLife.20795.

Azriel-Tamir, H., Sharir, H., Schwartz, B., Hershfinkel, M., 2004. Extracellular zinc triggers ERK-dependent activation of Na+/H+ exchange in colonocytes mediated by the zinc-sensing receptor. J. Biol. Chem. 279 (50), 51804–51816.

Bolick, D.T., Kolling, G.L., Moore 2nd, J.H., de Oliveira, L.A., Tung, K., Philipson, C., Guerrant, R.L., 2014. Zinc deficiency alters host response and pathogen virulence in a mouse model of enteroaggregative Escherichia coli-induced diarrhea. Gut Microbes 5 (5), 618–627. https://doi.org/10.4161/19490976.2014.969642.

Bolick, D.T., Medeiros, P., Ledwaba, S.E., Lima, A.A.M., Nataro, J.P., Barry, E.M., Guerrant, R.L., 2018. The Critical Role of Zinc in a New Murine Model of Enterotoxigenic E. coli (ETEC) Diarrhea. Infect. Immun. https://doi.org/10.1128/IAI.00183-18.

Bradford, M.M., 1976. A rapid and sensitive method for the quantitation of microgram quantities of protein utilizing the principle of protein-dye binding. Anal. Biochem. 72, 248–254.

Chi, Y., Li, K., Yan, Q., Koizumi, S., Shi, L., Takahashi, S., Yao, J., 2011. Nonsteroidal anti-inflammatory drug flufenamic acid is a potent activator of AMP-activated protein kinase. J. Pharmacol. Exp. Ther. 339 (1), 257–266. https://doi.org/10.1124/jpet.111.183020.

Cohen, L., Asraf, H., Sekler, I., Hershfinkel, M., 2012a. Extracellular pH regulates zinc signaling via an Asp residue of the zinc-sensing receptor (ZnR/GPR39). J. Biol. Chem. 287 (40), 33339–33350.

Cohen, L., Azriel-Tamir, H., Arotsker, N., Sekler, I., Hershfinkel, M., 2012b. Zinc sensing receptor signaling, mediated by GPR39, reduces butyrate-induced cell death in HT29 colonocytes via upregulation of clusterin. PLoS One 7 (4), e35482.

Cohen, L., Sekler, I., Hershfinkel, M., 2014. The zinc sensing receptor, ZnR/GPR39, controls proliferation and differentiation of colonocytes and thereby tight junction formation in the colon. Cell Death Dis. 5, e1307. https://doi.org/10.1038/cddis.2014.262.

Cote, C.D., Rasmussen, B.A., Duca, F.A., Zadeh-Tahmasebi, M., Baur, J.A., Daljeet, M., Lam, T.K., 2015. Resveratrol activates duodenal Sirt1 to reverse insulin resistance in rats through a neuronal network. Nat. Med. 21 (5), 498–505. https://doi.org/10.1038/nm.3821.

de Queiroz, C.A., Fonseca, S.G., Frota, P.B., Figueiredo, I.L., Aragao, K.S., Magalhaes, C.E., Oria, R.B., 2014. Zinc treatment ameliorates diarrhea and intestinal inflammation in undernourished rats. BMC Gastroenterol. 14, 136. https://doi.org/10.1186/1471-230X-14-136.

Duca, F.A., Cote, C.D., Rasmussen, B.A., Zadeh-Tahmasebi, M., Rutter, G.A., Filippi, B.M., Lam, T.K., 2015. Metformin activates a duodenal Ampk-dependent pathway to lower hepatic glucose production in rats. Nat. Med. 21 (5), 506–511. https://doi.org/10.1038/nm.3787.

Egerod, K.L., Holst, B., Petersen, P.S., Hansen, J.B., Mulder, J., Hokfelt, T., Schwartz, T.W., 2007. GPR39 splice variants versus antisense gene LYPD1: expression and regulation in gastrointestinal tract, endocrine pancreas, liver, and white adipose tissue. Mol. Endocrinol. 21 (7), 1685–1698. https://doi.org/10.1210/me.2007-0055.

Hardie, D.G., Schaffer, B.E., Brunet, A., 2016. AMPK: an energy-sensing pathway with multiple inputs and outputs. Trends Cell Biol. 26 (3), 190–201. https://doi.org/10.1016/j.tcb.2015.10.013.

Hering, N.A., Fromm, M., Schulzke, J.D., 2012. Determinants of colonic barrier function in inflammatory bowel disease and potential therapeutics. J. Physiol. 590 (5), 1035–1044. https://doi.org/10.1113/jphysiol.2011.224568.

Hershfinkel, M., 2018. The zinc sensing receptor, ZnR/GPR39, in health and disease. Int. J. Mol. Sci. 19 (2). https://doi.org/10.3390/ijms19020439.

Holst, B., Egerod, K.L., Schild, E., Vickers, S.P., Cheetham, S., Gerlach, L.O., Schwartz, T.W., 2007. GPR39 signaling is stimulated by zinc ions but not by obestatin.

Endocrinology 148 (1), 13–20. https://doi.org/10.1210/en.2006-0933.
Kim, N., Lee, J.O., Lee, H.J., Kim, H.I., Kim, J.K., Lee, Y.W., Kim, H.S., 2015. Endogenous ligand for GPR120, docosahexaenoic acid, exerts benign metabolic effects on the skeletal muscles via AMP-activated protein kinase pathway. J. Biol. Chem. 290 (33), 20438–20447. https://doi.org/10.1074/jbc.M115.657379.
Lamberti, L.M., Walker, C.L., Chan, K.Y., Jian, W.Y., Black, R.E., 2013. Oral zinc supplementation for the treatment of acute diarrhea in children: a systematic review and meta-analysis. Nutrients 5 (11), 4715–4740. https://doi.org/10.3390/nu5114715.
Lindenmayer, G.W., Stoltzfus, R.J., Prendergast, A.J., 2014. Interactions between zinc deficiency and environmental enteropathy in developing countries. Adv. Nutr. 5 (1), 1–6. https://doi.org/10.3945/an.113.004838.
Lodemann, U., Einspanier, R., Scharfen, F., Martens, H., Bondzio, A., 2013. Effects of zinc on epithelial barrier properties and viability in a human and a porcine intestinal cell culture model. Toxicol. Vitr. 27 (2), 834–843. https://doi.org/10.1016/j.tiv.2012.12.019.
Miao, W., Wu, X., Wang, K., Wang, W., Wang, Y., Li, Z., Peng, L., 2016. Sodium butyrate promotes reassembly of tight junctions in Caco-2 monolayers involving inhibition of MLCK/MLC2 pathway and phosphorylation of PKCbeta2. Int. J. Mol. Sci. 17 (10). https://doi.org/10.3390/ijms17101696.
Moran, B.M., Abdel-Wahab, Y.H., Vasu, S., Flatt, P.R., McKillop, A.M., 2016. GPR39 receptors and actions of trace metals on pancreatic beta cell function and glucose homoeostasis. Acta Diabetol. 53 (2), 279–293. https://doi.org/10.1007/s00592-015-0781-5.
Muanprasat, C., Wongkrasant, P., Satitsri, S., Moonwiriyakit, A., Pongkorpsakol, P., Mattaveewong, T., Chatsudthipong, V., 2015. Activation of AMPK by chitosan oligosaccharide in intestinal epithelial cells: mechanism of action and potential applications in intestinal disorders. Biochem. Pharmacol. 96 (3), 225–236. https://doi.org/10.1016/j.bcp.2015.05.016.
Ni Shuilleabhain, S., Mothersill, C., Sheehan, D., O'Brien, N.M., J, O. H, Van Pelt, F.N., Davoren, M., 2004. In vitro cytotoxicity testing of three zinc metal salts using established fish cell lines. Toxicol. Vitr. 18 (3), 365–376. https://doi.org/10.1016/j.tiv.2003.10.006.
Odenwald, M.A., Choi, W., Buckley, A., Shashikanth, N., Joseph, N.E., Wang, Y., Turner, J.R., 2017. ZO-1 interactions with F-actin and occludin direct epithelial polarization and single lumen specification in 3D culture. J. Cell Sci. 130 (1), 243–259. https://doi.org/10.1242/jcs.188185.
Park, J.S., Choi, J., Kwon, J.Y., Jung, K.A., Yang, C.W., Park, S.H., Cho, M.L., 2018. A probiotic complex, rosavin, zinc, and prebiotics ameliorate intestinal inflammation in an acute colitis mouse model. J. Transl. Med. 16 (1), 37. https://doi.org/10.1186/s12967-018-1410-1.
Patel, A.B., Mamtani, M., Badhoniya, N., Kulkarni, H., 2011. What zinc supplementation does and does not achieve in diarrhea prevention: a systematic review and meta-analysis. BMC Infect. Dis. 11, 122. https://doi.org/10.1186/1471-2334-11-122.
Pavlica, S., Gaunitz, F., Gebhardt, R., 2009. Comparative in vitro toxicity of seven zinc-salts towards neuronal PC12 cells. Toxicol. Vitr. 23 (4), 653–659. https://doi.org/10.1016/j.tiv.2009.03.003.
Peng, L., Li, Z.R., Green, R.S., Holzman, I.R., Lin, J., 2009. Butyrate enhances the intestinal barrier by facilitating tight junction assembly via activation of AMP-activated protein kinase in Caco-2 cell monolayers. J. Nutr. 139 (9), 1619–1625. https://doi.org/10.3945/jn.109.104638.
Petersen, P.S., Jin, C., Madsen, A.N., Rasmussen, M., Kuhre, R., Egerod, K.L., Holst, B., 2011. Deficiency of the GPR39 receptor is associated with obesity and altered adipocyte metabolism. FASEB J. 25 (11), 3803–3814. https://doi.org/10.1096/fj.11-184531.
Peukert, S., Hughes, R., Nunez, J., He, G., Yan, Z., Jain, R., Bose, A., 2014. Discovery of 2-pyridylpyrimidines as the first orally bioavailable GPR39 agonists. ACS Med. Chem. Lett. 5 (10), 1114–1118. https://doi.org/10.1021/ml500240d.
Pongkorpsakol, P., Moonwiriyakit, A., Muanprasat, C., 2017a. Fatty acid and mineral receptors as drug targets for gastrointestinal disorders. Future Med Chem. 9 (3), 315–334. https://doi.org/10.4155/fmc-2016-0205.
Pongkorpsakol, P., Satitsri, S., Wongkrasant, P., Chittavanich, P., Kittayaruksakul, S., Srimanote, P., Muanprasat, C., 2017b. Flufenamic acid protects against intestinal fluid secretion and barrier leakage in a mouse model of Vibrio cholerae infection through NF-kappaB inhibition and AMPK activation. Eur. J. Pharmacol. 798, 94–104. https://doi.org/10.1016/j.ejphar.2017.01.026.
Salminen, A., Hyttinen, J.M., Kaarniranta, K., 2011. AMP-activated protein kinase inhibits NF-kappaB signaling and inflammation: impact on healthspan and lifespan. J. Mol. Med. 89 (7), 667–676. https://doi.org/10.1007/s00109-011-0748-0.
Satitsri, S., Pongkorpsakol, P., Srimanote, P., Chatsudthipong, V., Muanprasat, C., 2016. Pathophysiological mechanisms of diarrhea caused by the Vibrio cholerae O1 El Tor variant: an in vivo study in mice. Virulence 7 (7), 789–805. https://doi.org/10.1080/21505594.2016.1192743.
Shao, Y., Wolf, P.G., Guo, S., Guo, Y., Gaskins, H.R., Zhang, B., 2017a. Zinc enhances intestinal epithelial barrier function through the PI3K/AKT/mTOR signaling pathway in Caco-2 cells. J. Nutr. Biochem. 43, 18–26. https://doi.org/10.1016/j.jnutbio.2017.01.013.
Shao, Y.X., Lei, Z., Wolf, P.G., Gao, Y., Guo, Y.M., Zhang, B.K., 2017b. Zinc Supplementation, via GPR39, Upregulates PKCzeta to Protect Intestinal Barrier Integrity in Caco-2 Cells Challenged by Salmonella enterica Serovar Typhimurium. J. Nutr. 147 (7), 1282–1289. https://doi.org/10.3945/jn.116.243238.
Shimizu, Y., Koyama, R., Kawamoto, T., 2017. Rho kinase-dependent desensitization of GPR39; a unique mechanism of GPCR downregulation. Biochem. Pharmacol. 140, 105–114. https://doi.org/10.1016/j.bcp.2017.06.115.
Strober, W., Fuss, I., Mannon, P., 2007. The fundamental basis of inflammatory bowel disease. J. Clin. Investig. 117 (3), 514–521. https://doi.org/10.1172/JCI30587.
Sungkaworn, T., Lenbury, Y., Chatsudthipong, V., 2011. Oxidative stress increases angiotensin receptor type I responsiveness by increasing receptor degree of aggregation using image correlation spectroscopy. Biochim. Biophys. Acta 1808 (10), 2496–2500. https://doi.org/10.1016/j.bbamem.2011.07.007.
Sunuwar, L., Medini, M., Cohen, L., Sekler, I., Hershfinkel, M., 2016. The zinc sensing receptor, ZnR/GPR39, triggers metabotropic calcium signalling in colonocytes and regulates occludin recovery in experimental colitis. Philos. Trans. R. Soc. Lond. B Biol. Sci. 371 (1700). https://doi.org/10.1098/rstb.2015.0420.
Terrin, G., Berni Canani, R., Di Chiara, M., Pietravalle, A., Aleandri, V., Conte, F., De Curtis, M., 2015. Zinc in early life: a Key element in the fetus and preterm neonate. Nutrients 7 (12), 10427–10446. https://doi.org/10.3390/nu7125542.
Thiagarajah, J.R., Donowitz, M., Verkman, A.S., 2015. Secretory diarrhoea: mechanisms and emerging therapies. Nat. Rev. Gastroenterol. Hepatol. 12 (8), 446–457. https://doi.org/10.1038/nrgastro.2015.111.
Tuerk, M.J., Fazel, N., 2009. Zinc deficiency. Curr. Opin. Gastroenterol. 25 (2), 136–143. https://doi.org/10.1097/MOG.0b013e328321b395.
Yano, T., Matsui, T., Tamura, A., Uji, M., Tsukita, S., 2013. The association of microtubules with tight junctions is promoted by cingulin phosphorylation by AMPK. J. Cell Biol. 203 (4), 605–614. https://doi.org/10.1083/jcb.201304194.
Yasuda, S., Miyazaki, T., Munechika, K., Yamashita, M., Ikeda, Y., Kamizono, A., 2007. Isolation of Zn2+ as an endogenous agonist of GPR39 from fetal bovine serum. J. Recept. Signal Transduct. Res. 27 (4), 235–246. https://doi.org/10.1080/10799890701506147.
Yousef, M., Pichyangkura, R., Soodvilai, S., Chatsudthipong, V., Muanprasat, C., 2012. Chitosan oligosaccharide as potential therapy of inflammatory bowel disease: therapeutic efficacy and possible mechanisms of action. Pharmacol. Res. 66 (1), 66–79. https://doi.org/10.1016/j.phrs.2012.03.013.
Zakrzewski, S.S., Fromm, M., Schulzke, J.D., Gunzel, D., 2017. Zinc strengthens the jejunal barrier by reversibly tightening the paracellular route. Am. J. Physiol. Gastrointest. Liver Physiol. 313 (6), G537–G548. https://doi.org/10.1152/ajpgi.00355.2016.
Zhang, L., Li, J., Young, L.H., Caplan, M.J., 2006. AMP-activated protein kinase regulates the assembly of epithelial tight junctions. Proc. Natl. Acad. Sci. USA 103 (46), 17272–17277. https://doi.org/10.1073/pnas.0608531103.
Zheng, B., Cantley, L.C., 2007. Regulation of epithelial tight junction assembly and disassembly by AMP-activated protein kinase. Proc. Natl. Acad. Sci. USA 104 (3), 819–822. https://doi.org/10.1073/pnas.0610157104.